

Table S1. Global and regional soil carbon datasets and their source

Global and regional datasets	
Identifier	Source
Canada National Pedon Database - NPDB	Agriculture and Agri-Food Canada, Government of Canada. National Pedon Database. https://open.canada.ca/data/en/dataset/6457fad6-b6f5-47a3-9bd1-ad14aea4b9e0 , 2021.
Global ISRIC WISE30sec v.3.	Batjes, N. H.: Harmonized soil property values for broad-scale modelling (WISE30sec) with estimates of global soil carbon stocks, <i>Geoderma</i> , 269, 61–68, https://doi.org/10.1016/j.geoderma.2016.01.034 , 2016.
China tropical montane dataset	de Blécourt, M., Corre, M. D., Paudel, E., Harrison, R. D., Brumme, R., and Veldkamp, E.: Spatial variability in soil organic carbon in a tropical montane landscape: associations between soil organic carbon and land use, soil properties, vegetation, and topography vary across plot to landscape scales, <i>SOIL</i> , 3, 123–137, https://doi.org/10.5194/soil-3-123-2017 , 2017.
Global WoSIS snapshot December 2023	Calisto, L., de Sousa, L.M., and Batjes, N.H. Standardised soil profile data for the world (WoSIS snapshot – December 2023), https://doi.org/10.17027/isric-wdcsoils-20231130 , 2023. Batjes, N. H., Calisto, L., and de Sousa, L. M.: Providing quality-assessed and standardised soil data to support global mapping and modelling (WoSIS snapshot 2023), <i>Earth System Science Data Discussions</i> , 2024, 1–46, https://doi.org/10.5194/essd-2024-14 , 2024.
Europe, LUCAS 2018 topsoil data	Fernandez-Ugalde, O; Scarpa, S; Orgiazzi, A.; Panagos, P.; Van Liedekerke, M; Marechal A. and Jones, A. LUCAS 2018 Soil Module. Presentation of dataset and results, EUR 31144 EN, Publications Office of the European Union, Luxembourg. ISBN 978-92-76-54832-4, doi:10.2760/215013, JRC129926, 2022. https://esdac.jrc.ec.europa.eu/content/lucas-2018-topsoil-data
Mexico	Guevara, M., Arroyo, C., Brunsell, N., Cruz, C. O., Domke, G., Equihua, J., Etchevers, J., Hayes, D., Hengl, T., Ibelles, A., Johnson, K., de Jong, B., Libohova, Z., Llamas, R., Nave, L., Ornelas, J. L., Paz, F., Ressl, R., Schwartz, A., Victoria, A., Wills, S., and Vargas, R.: Soil Organic Carbon Across Mexico and the Conterminous United States (1991–2010), <i>Global Biogeochemical Cycles</i> , 34, e2019GB006219, https://doi.org/10.1029/2019GB006219 , 2020. Krasilnikov, P., Gutiérrez-Castorena, M. d. C., Ahrens, R. J., Cruz-Gaistardo, C. O., Sedov, S., and Solleiro-Rebolledo, E. <i>The Soils of Mexico</i> . Dordrecht: Springer Netherlands, 2013.
Chile – CLSoilMaps dataset, included in WoSIS dataset	Dinamarca, D. I., Galleguillos, M., Seguel, O., and Faúndez Urbina, C.: CLSoilMaps: A national soil gridded database of physical and hydraulic soil properties for Chile, <i>Scientific Data</i> , 10, 630, https://doi.org/10.1038/s41597-023-02536-x , 2023.
Ecuador HESD	Armas, D.I., M. Guevara, F. Bezares, R. Vargas, P. Durante, V.H. Osorio, W.A. Jimenez, and Oyonarte, C. Harmonized Soil Database of Ecuador 2021 ver 3. Environmental Data Initiative. https://doi.org/10.6073/pasta/1560e803953c839e7aedef78ff7d3f6c , 2022.
Brazil	MapBiomass: Annual mapping of soil organic carbon stock in Brazil 1985–2021 (beta collection). Training field soil data (V1), https://doi.org/10.60502/SoilData/XDBQ4U , 2023.
International Soil Carbon Network v.3. database (ISCN)	Nave, L., K. Johnson, C. van Ingen, D. Agarwal, M. Humphrey, and Beekwilder, N. International Soil Carbon Network version 3 Database (ISCN3) ver 1. Environmental Data Initiative. https://doi.org/10.6073/pasta/cc751923c5576b95a6d6a227d5afe8ba , 2022.
United States, Rapid Carbon Assessment (RaCA)	Soil Survey Staff. Rapid Carbon Assessment (RaCA) project. United States Department of Agriculture, Natural Resources Conservation Service. Available online. https://nrcs.app.box.com/s/s9bcdroihv1vyre70bkl336cdr13up7q , 2013.
Guatemala	Vásquez-Toxcón, A. O., Tobías Vásquez, H., and Guevara, M. Guatemala Soil Organic Carbon Database (0 to 30 cm, 1965–2010). ver 1. Environmental Data Initiative. https://doi.org/10.6073/pasta/8dd15238c604c3ac75daf985548bd05c , 2023.

Table S2. Ecosystem-specific soil carbon datasets and their source

<u>System-specific datasets</u>	
Identifier	Source
Southeast Asia, baseline samples were used	Gomez, F., Carcedo, A., Mean, C. M., Reyes, M., Hok, L., Tivet, F., Seng, V., Vara Prasad, P. V., and Ciampitti, I.: A dataset for soil organic carbon in agricultural systems for the Southeast Asia region, <i>Scientific Data</i> , 11, 374, https://doi.org/10.1038/s41597-024-03213-3 , 2024.
Permafrost, Northern Circumpolar Soil Carbon dataset (NCSCDv2)	Hugelius, G., Bockheim, J. G., Camill, P., Elberling, B., Grosse, G., Harden, J. W., Johnson, K., Jorgenson, T., Koven, C. D., Kuhry, P., Michaelson, G., Mishra, U., Palmtag, J., Ping, C.-L., O'Donnell, J., Schirrmeyer, L., Schuur, E. A. G., Sheng, Y., Smith, L. C., Strauss, J., and Yu, Z.: A new data set for estimating organic carbon storage to 3 m depth in soils of the northern circumpolar permafrost region, <i>Earth System Science Data</i> , 5, 393–402, https://doi.org/10.5194/essd-5-393-2013 , 2013.
Marshlands, MarSOC	Maxwell, T. L., Rovai, A. S., Adame, M. F., Adams, J. B., Álvarez-Rogel, J., Austin, W. E. N., Beasy, K., Boscutti, F., Böttcher, M. E., Bouma, T. J., Bulmer, R. H., Burden, A., Burke, S. A., Camacho, S., Chaudhary, D. R., Chmura, G. L., Copertino, M., Cott, G. M., Craft, C., Day, J., de los Santos, C. B., Denis, L., Ding, W., Ellison, J. C., Ewers Lewis, C. J., Giani, L., Gispert, M., Gonthonet, S., González-Pérez, J. A., González-Alcaraz, M. N., Gorham, C., Graversen, A. E. L., Grey, A., Guerra, R., He, Q., Holmquist, J. R., Jones, A. R., Juanes, J. A., Kelleher, B. P., Kohfeld, K. E., Krause-Jensen, D., Lafratta, A., Lavery, P. S., Laws, E. A., Leiva-Dueñas, C., Loh, P. S., Lovelock, C. E., Lundquist, C. J., Macreadie, P. I., Mazarrasa, I., Megonigal, J. P., Neto, J. M., Nogueira, J., Osland, M. J., Pagès, J. F., Perera, N., Pfeiffer, E.-M., Pollmann, T., Raw, J. L., Recio, M., Ruiz-Fernández, A. C., Russell, S. K., Rybczyk, J. M., Sammul, M., Sanders, C., Santos, R., Serrano, O., Siewert, M., Smeaton, C., Song, Z., Trasar-Cepeda, C., Twilley, R. R., Van de Broek, M., Vitti, S., Antisari, L. V., Voltz, B., Wails, C. N., Ward, R. D., Ward, M., Wolfe, J., Yang, R., Zubrzycki, S., Landis, E., Smart, L., Spalding, M., and Worthington, T. A.: Global dataset of soil organic carbon in tidal marshes, <i>Scientific Data</i> , 10, 797, https://doi.org/10.1038/s41597-023-02633-x , 2023.
Permafrost, Sweden	Siewert, M. B.: High-resolution digital mapping of soil organic carbon in permafrost terrain using machine learning: a case study in a sub-Arctic peatland environment, <i>Biogeosciences</i> , 15(6), 1663–1683, https://doi.org/10.5194/bg-15-1663-2018 , 2018.
Forested wetland soils, ‘cryptic carbon’ dataset	Stewart, A. J., Halabisky, M., Babcock, C., Butman, D. E., D’Amore, D. V., and Moskal, L. M.: Revealing the hidden carbon in forested wetland soils, <i>Nature Communications</i> , 15, 726, https://doi.org/10.1038/s41467-024-44888-x , 2024.

Table S2. Ecosystem-specific soil carbon datasets and their source (continued)

<u>System-specific datasets (continued)</u>	
<u>Mangrove datasets</u>	
Identifier	Source
Mangrove, Demak, Indonesia, SWAMP-CIFOR	Ardhani, T. S. P., Murdiyarso, D., and Kusmana, C.: SWAMP Dataset-Soil-Demak-2019 (V1), https://doi.org/10.17528/CIFOR/DATA.00282 , 2021.
Mangrove, Berahan kulon, SWAMP-CIFOR	Ardhani, T. S. P., Murdiyarso, D., and Kusmana, C.: SWAMP Dataset-Soil-Demak-2019 (V1), https://doi.org/10.17528/CIFOR/DATA.00282 , 2021.
Mangroves	Atwood, T., Connolly, R. M., Almahaesheer, H., Carnell, P., Duarte, C. M., Lewis, C. E., Irigoien, X., Kelleway, J., Lavery, P. S., Macreadie, P. I., Serrano, Ó., Sanders, I., Santos, I. R., Steven, S., and Lovelock, C. E.: Country-level mangrove soil carbon stocks and losses, https://doi.org/10.1594/PANGAEA.874382 , 2017.
Mangrove, Acarau Boca, Brazil, SWAMP-CIFOR	Kauffman, J. B., Bernardino, A. F., Ferreira, T. O., Giovannoni, L. R., de O. Gomes, L. E., Romero, D. J., Jimenez, L. C. Z., and Ruiz, F.: SWAMP Dataset-Mangrove soil carbon-Acarau Boca-2016 (V1), https://doi.org/10.17528/CIFOR/DATA.00171 , 2019.
Mangrove, SWAMP-CIFOR	Kauffman, J. B. and Bhomia, R. K.: SWAMP Dataset-Mangrove soil carbon-Gabon North-2014 (V1), https://doi.org/10.17528/CIFOR/DATA.00215 , 2020.
Mangrove, Bunaken, Indonesia, SWAMP-CIFOR	Murdiyarso, D., Purbopuspito, J., Kauffman, J. B., Warren, M. W., Sasmito, S. D., Manuri, S., Krisnawati, H., Taberima, S., and Kurnianto, S.: SWAMP Dataset-Mangrove soil carbon-Bunaken-2011 (V1), https://doi.org/10.17528/CIFOR/DATA.00141 , 2019a.
Mangrove, Kubu Raya, Indonesia, SWAMP-CIFOR	Murdiyarso, D., Purbopuspito, J., Kauffman, J. B., Warren, M. W., Sasmito, S. D., Manuri, S., Krisnawati, H., Taberima, S., and Kurnianto, S.: SWAMP Dataset-Mangrove soil carbon-Kubu Raya-2011 (V1), https://doi.org/10.17528/CIFOR/DATA.00143 , 2019b.
Mangrove, Sembilang, Indonesia, SWAMP-CIFOR	Murdiyarso, D., Purbopuspito, J., Kauffman, J. B., Warren, M. W., Sasmito, S. D., Manuri, S., Krisnawati, H., Taberima, S., and Kurnianto, S.: SWAMP Dataset-Mangrove soil carbon-Sembilang-2011 (V1), https://doi.org/10.17528/CIFOR/DATA.00144 , 2019c.
Mangrove, Teminabuan, Indonesia, SWAMP-CIFOR	Murdiyarso, D., Purbopuspito, J., Kauffman, J. B., Warren, M. W., Sasmito, S. D., Manuri, S., Krisnawati, H., Taberima, S., and Kurnianto, S.: SWAMP Dataset-Mangrove soil carbon-Teminabuan-2011 (V1), https://doi.org/10.17528/CIFOR/DATA.00146 , 2019d.
Mangrove, Timika, Indonesia, SWAMP-CIFOR	Murdiyarso, D., Purbopuspito, J., Kauffman, J. B., Warren, M. W., Sasmito, S. D., Manuri, S., Krisnawati, H., Taberima, S., and Kurnianto, S.: SWAMP Dataset-Mangrove soil carbon-Timika-2011 (V1), https://doi.org/10.17528/CIFOR/DATA.00147 , 2019e.
Mangroves, TNC-WHRC	Sanderman, J., Hengl, T., Fiske, G., Solvik, K., Adame, M. F., Benson, L., Bukoski, J. J., Carnell, P., Cifuentes-Jara, M., Donato, D., Duncan, C., Eid, E. M., Ermgassen, P. zu, Lewis, C. J. E., Macreadie, P. I., Glass, L., Gress, S., Jardine, S. L., Jones, T. G., Nsombo, E. N., Rahman, M. M., Sanders, C. J., Spalding, M., and Landis, E.: A global map of mangrove forest soil carbon at 30 m spatial resolution, <i>Environmental Research Letters</i> , 13, 055002, https://doi.org/10.1088/1748-9326/aabe1c , 2018.
Mangrove, West Papua, SWAMP-CIFOR	Sasmito, S. D., Silanpää, M., Hayes, M. A., Bachri, S., Saragi-Sasmito, M. F., Sidik, F., Hanggara, B., Mofu, W. Y., Rumbiak, V. I., Hendri, Rumbiak, M. I., Taberima, S., Suhaemi, Nugroho, J. D., Pattiasina, T. F., Widagti, N., Barakalla, Rahajoe, J. S., Hartantri, H., Nikijuluw, V., Jowey, R. N., Heatunubun, C., Ermgassen, P. z., Worthington, T. A., Howard, J., Lovelock, C. E., Friess, D. A., Hutley, L. B., and Murdiyarso, D.: SWAMP Dataset-Mangrove biomass vegetation-West Papua-2019 (V2), https://doi.org/10.17528/CIFOR/DATA.00193 , 2019.
Mangrove, Ca Mau, Vietnam, SWAMP-CIFOR	Vien, N. N., Sasmito, S. D., Murdiyarso, D., Purbopuspito, J., and MacKenzie, R. A.: SWAMP Dataset-Mangrove soil carbon-Ca Mau-2012 (V1), https://doi.org/10.17528/CIFOR/DATA.00149 , 2019a.
Mangrove, Can Gio, Vietnam, SWAMP-CIFOR	Vien, N. N., Sasmito, S. D., Murdiyarso, D., Purbopuspito, J., and MacKenzie, R. A.: SWAMP Dataset-Mangrove soil carbon-Can Gio-2012 (V1), https://doi.org/10.17528/CIFOR/DATA.00148 , 2019b.

Table S2. Ecosystem-specific soil carbon datasets and their source (continued)

System-specific datasets (continued)	
Peatland datasets	
Identifier	Source
Peatlands, Kalimantan, Indonesia	Anshari, G. Z., Afifudin, M., Nuriman, M., Gusmayanti, E., Arianie, L., Susana, R., Nusantara, R. W., Sugardjito, J., and Rafiastanto, A.: Drainage and land use impacts on changes in selected peat properties and peat degradation in West Kalimantan Province, Indonesia, <i>Biogeosciences</i> , 7, 3403-3419, https://doi.org/10.5194/bg-7-3403-2010 , 2010.
Peatlands, Congo Basin	Crezee, B., Dargie, G. C., Ewango, C. E. N., Mitchard, E. T. A., Emba B., O., Kanyama T., J., Bola, P., Ndjango, J.-B. N., Girkin, N. T., Bocko, Y. E., Ifo, S. A., Hubau, W., Seidensticker, D., Batumike, R., Imani, G., Cuni-Sanchez, A., Kiahtipes, C. A., Lebambo, J., Wotzka, H.-P., Bean, H., Baker, T. R., Baird, A. J., Boom, A., Morris, P. J., Page, S. E., Lawson, I. T., and Lewis, S. L.: Mapping peat thickness and carbon stocks of the central Congo Basin using field data, <i>Nature Geoscience</i> , 15, 639–644, https://doi.org/10.1038/s41561-022-00966-7 , 2022.
Peatlands, Papua, Indonesia	Gani, R. A., Barus, P. A., and Sukarman: Properties and carbon stocks of tropical tidal peat soils deposited on coral limestone in Numfor and Supiori Islands, Papua Province, <i>IOP Conference Series: Earth and Environmental Science</i> , 648, 012001, https://doi.org/10.1088/1755-1315/648/1/012001 , 2021.
Peatlands, Malaysia	Sangok, F. E., Sugiura, Y., Maie, N., Melling, L., Nakamura, T., Ikeya, K., and Watanabe, A.: Variations in the rate of accumulation and chemical structure of soil organic matter in a coastal peatland in Sarawak, Malaysia, <i>CATENA</i> , 184, 104244, https://doi.org/10.1016/j.catena.2019.104244 , 2020.
Peatland, Katingan, Indonesia, SWAMP-CIFOR	Saragi-Sasmito, M. F., Murdiyarsa, D., June, T., and Austin, K. G.: SWAMP Dataset-Peatland soil carbon-Katingan-2015, https://doi.org/10.17528/CIFOR/DATA.00093 , 2015.
Peatlands, Kalimantan, Indonesia	Shimada, S., Takahashi, H., Haraguchi, A., and Kaneko, M.: The carbon content characteristics of tropical peats in Central Kalimantan, Indonesia: Estimating their spatial variability in density, <i>Biogeochemistry</i> , 53, 249-267, https://doi.org/10.1023/A:1010618807469 , 2001.

Table S3. High-confidence gridded datasets that were integrated into our analysis

Gridded datasets		
Country	Layers	Source
Congo Basin peatlands	topsoil and subsoil	Crezee, B., Dargie, G. C., Ewango, C. E. N., Mitchard, E. T. A., Emba B., O., Kanyama T., J., Bola, P., Ndjango, J.-B. N., Girkin, N. T., Bocko, Y. E., Ifo, S. A., Hubau, W., Seidensticker, D., Batumike, R., Imani, G., Cuni-Sanchez, A., Kiahtipes, C. A., Lebamba, J., Wotzka, H.-P., Bean, H., Baker, T. R., Baird, A. J., Boom, A., Morris, P. J., Page, S. E., Lawson, I. T., and Lewis, S. L.: Mapping peat thickness and carbon stocks of the central Congo Basin using field data, <i>Nature Geoscience</i> , 15, 639–644, https://doi.org/10.1038/s41561-022-00966-7 , 2022.
Peru peatlands	topsoil and subsoil	Hastie, A., Honorio Coronado, E. N., Reyna, J., Mitchard, E. T. A., Åkesson, C. M., Baker, T. R., Cole, L. E. S., Oroche, César. J. C., Dargie, G., Dávila, N., De Grandi, E. C., Del Águila, J., Del Castillo Torres, D., De La Cruz Paiva, R., Draper, F. C., Flores, G., Grández, J., Hergoualc'h, K., Householder, J. E., Janovec, J. P., Lähteenoja, O., Reyna, D., Rodríguez-Veiga, P., Roucoux, K. H., Tobler, M., Wheeler, C. E., Williams, M., and Lawson, I. T.: Risks to carbon storage from land-use change revealed by peat thickness maps of Peru, <i>Nature Geoscience</i> , 15, 369–374, https://doi.org/10.1038/s41561-022-00923-4 , 2022.
Tanzania	topsoil	Kempen, B., Dalsgaard, S., Kaaya, A. K., Chamuya, N., Ruipérez-González, M., Pekkarinen, A., and Walsh, M. G.: Mapping topsoil organic carbon concentrations and stocks for Tanzania, <i>Geoderma</i> , 337, 164–180, https://doi.org/10.1016/j.geoderma.2018.09.011 , 2019.
South Africa	topsoil	Venter, Z. S., Hawkins, H.-J., Cramer, M. D., and Mills, A. J.: Mapping soil organic carbon stocks and trends with satellite-driven high resolution maps over South Africa, <i>Science of The Total Environment</i> , 771, 145384, https://doi.org/10.1016/j.scitotenv.2021.145384 , 2021.
Global mangrove regions	topsoil and subsoil	Sanderman, J., Hengl, T., Fiske, G., Solvik, K., Adame, M. F., Benson, L., Bukoski, J. J., Carnell, P., Cifuentes-Jara, M., Donato, D., Duncan, C., Eid, E. M., Ermgassen, P. zu, Lewis, C. J. E., Macreadie, P. I., Glass, L., Gress, S., Jardine, S. L., Jones, T. G., Nsombo, E. N., Rahman, M. M., Sanders, C. J., Spalding, M., and Landis, E.: A global map of mangrove forest soil carbon at 30 m spatial resolution, <i>Environmental Research Letters</i> , 13, 055002, https://doi.org/10.1088/1748-9326/aabe1c , 2018.
Australia	topsoil	Viscarra Rossel, R., Webster, R., Bui, E., and Baldock, J.: Baseline map of Australian soil organic carbon stocks and their uncertainty. v2. CSIRO. Data Collection. https://doi.org/10.4225/08/556BCD6A38737 , 2014.
Third Pole region	topsoil and subsoil	Wang, D., Wu, T., Zhao, L., Mu, C., Li, R., Wei, X., Hu, G., Zou, D., Zhu, X., Chen, J., Hao, J., Ni, J., Li, X., Ma, W., Wen, A., Shang, C., La, Y., Ma, X., and Wu, X.: A 1km resolution soil organic carbon dataset for frozen ground in the Third Pole, <i>Earth System Science Data</i> , 13, 3453–3465, https://doi.org/10.5194/essd-13-3453-2021 , 2021.

Table S4. Remote-sensing datasets & Environmental covariates

Remote-sensing datasets & Environmental covariates	
Identifier	Source
Global bare cover fraction - Copernicus Global Land Cover Layers - CGLS-LC100 Collection 3	Buchhorn, M., Lesiv, M., Tsednbazar, N.-E., Herold, M., Bertels, L., and Smets, B.: Copernicus Global Land Cover Layers—Collection 2, <i>Remote Sensing</i> , 12, https://doi.org/10.3390/rs12061044 , 2020.
Global 30m Digital Elevation Model (DEM)	COPERNICUS/DEM/GLO30
ISRIC global soil CEC, pH, nitrogen, sand, silt and clay at 30cm and 100cm	Hengl, T., Mendes de Jesus, J., Heuvelink, G. B. M., Ruijper Gonzalez, M., Kilibarda, M., Blagotić, A., Shangguan, W., Wright, M. N., Geng, X., Bauer-Marschallinger, B., Guevara, M. A., Vargas, R., MacMillan, R. A., Batjes, N. H., Leenaars, J. G. B., Ribeiro, E., Wheeler, I., Mantel, S., and Kempen, B.: SoilGrids250m: Global gridded soil information based on machine learning, <i>PLOS ONE</i> , 12, 1–40, https://doi.org/10.1371/journal.pone.0169748 , 2017.
Landsat 8, bands red, NiR, SWIR1 and SWIR2 - median of year 2022	LANDSAT/LC08/C02/T1_L2 - USGS
LST_day and night (unit: K) - Terra Land Surface Temperature and Emissivity 8-Day Global - 1 km native resolution - mean of 2000-02-18 to 2024-01-01	MODIS/061/MOD11A2 - NASA LP DAAC at the USGS EROS Center
Modis Evapotranspiration (ET) (unit: kg/m ² /8day) - Terra Net Evapotranspiration Gap-Filled 8-Day Global mean of 2000-01-01 to 2022-12-27	MODIS/061/MOD16A2GF - NASA LP DAAC at the USGS EROS Center
Fire frequency (burnt days/year) – annual average for the time range: 2000-11-01 to 2023-11-01 – native resolution is 500m	MODIS/061/MCD64A1
ALOS PALSAR HH and HV bands (unitless) - median of years 2019-2020 - JAXA/ALOS/PALSAR/YEARLY/SAR - JAXA EORC	Shimada, M., Itoh, T., Motooka, T., Watanabe, M., Shiraishi, T., Thapa, R., and Lucas, R.: New global forest/non-forest maps from ALOS PALSAR data (2007–2010), <i>Remote Sensing of Environment</i> , 155, 13–31, https://doi.org/10.1016/j.rse.2014.04.014 , 2014.

Table S5. Categorical datasets used for model training

<u>Categorical datasets</u>	
<u>Identifier</u>	<u>Source</u>
Mask for ocean, permanent water bodies and snow cover - Copernicus Global Land Cover Layers: CGLS-LC100 Collection 3	Buchhorn, M., Lesiv, M., Tsednbazar, N.-E., Herold, M., Bertels, L., and Smets, B.: Copernicus Global Land Cover Layers—Collection 2, <i>Remote Sensing</i> , 12, https://doi.org/10.3390/rs12061044 , 2020.
Global Mangrove Watch v.3.0, year 2020	Bunting, P., Rosenvist, A., Hilarides, L., Lucas, R. M., Thomas, N., Tadono, T., Worthington, T. A., Spalding, M., Murray, N. J., and Rebelo, L.-M.: Global Mangrove Extent Change 1996–2020: Global Mangrove Watch Version 3.0, <i>Remote Sensing</i> , 14, https://doi.org/10.3390/rs14153657 , 2022.
Congo Basin peatlands	Crezee, B., Dargie, G. C., Ewango, C. E. N., Mitchard, E. T. A., Emba B., O., Kanyama T., J., Bola, P., Ndjango, J.-B. N., Girkin, N. T., Bocko, Y. E., Ifo, S. A., Hubau, W., Seidensticker, D., Batumike, R., Imani, G., Cuní-Sánchez, A., Kiahtipes, C. A., Lebamba, J., Wotzka, H.-P., Bean, H., Baker, T. R., Baird, A. J., Boom, A., Morris, P. J., Page, S. E., Lawson, I. T., and Lewis, S. L.: Mapping peat thickness and carbon stocks of the central Congo Basin using field data, <i>Nature Geoscience</i> , 15, 639–644, https://doi.org/10.1038/s41561-022-00966-7 , 2022.
Peru peatlands	Hastie, A., Honorio Coronado, E. N., Reyna, J., Mitchard, E. T. A., Åkesson, C. M., Baker, T. R., Cole, L. E. S., Oroche, César. J. C., Dargie, G., Dávila, N., De Grandi, E. C., Del Águila, J., Del Castillo Torres, D., De La Cruz Paiva, R., Draper, F. C., Flores, G., Grández, J., Hergoualc'h, K., Householder, J. E., Janovec, J. P., Lähteenoja, O., Reyna, D., Rodriguez-Veiga, P., Roucoux, K. H., Tobler, M., Wheeler, C. E., Williams, M., and Lawson, I. T.: Risks to carbon storage from land-use change revealed by peat thickness maps of Peru, <i>Nature Geoscience</i> , 15, 369–374, https://doi.org/10.1038/s41561-022-00923-4 , 2022.
WRB 2006 subgroup classes – SoilGrids250m 2017-03	Hengl, T., Mendes de Jesus, J., Heuvellink, G. B. M., Ruijper Gonzalez, M., Kilibarda, M., Blagotić, A., Shangguan, W., Wright, M. N., Geng, X., Bauer-Marschallinger, B., Guevara, M. A., Vargas, R., MacMillan, R. A., Batjes, N. H., Leenaars, J. G. B., Ribeiro, E., Wheeler, I., Mantel, S., and Kempen, B.: SoilGrids250m: Global gridded soil information based on machine learning, <i>PLOS ONE</i> , 12, 1–40, https://doi.org/10.1371/journal.pone.0169748 , 2017.
Permafrost - NCSCDv2 Circumpolar permafrost region extent – native resolution is 0.012 deg.	Hugelius, G., Tarnocai, C., Broll, G., Canadell, J. G., Kuhry, P., and Swanson, D. K.: The Northern Circumpolar Soil Carbon Database: spatially distributed datasets of soil coverage and soil carbon storage in the northern permafrost regions, <i>Earth System Science Data</i> , 5, 3–13, https://doi.org/10.5194/essd-5-3-2013 , 2013.
WWF ecoregions	Olson, D. M., Dinerstein, E., Wikramanayake, E. D., Burgess, N. D., Powell, G. V. N., Underwood, E. C., D'amico, J. A., Itoua, I., Strand, H. E., Morrison, J. C., Loucks, C. J., Allnutt, T. F., Ricketts, T. H., Kura, Y., Lamoreux, J. F., Wettenberg, W. W., Hedao, P., and Kassem, K. R.: Terrestrial Ecoregions of the World: A New Map of Life on Earth: A new global map of terrestrial ecoregions provides an innovative tool for conserving biodiversity, <i>BioScience</i> , 51, 933–938, https://doi.org/10.1641/0006-3568(2001)051[0933:TEOTWA]2.0.CO;2 , 2001.
Greifswald Mire Center - Global Peatland Assessment (GPA) Database 2022 v.2	UNEP: Global Peatlands Assessment – The State of the World's Peatlands: Evidence for action toward the conservation, restoration, and sustainable management of peatlands. Main Report. Global Peatlands Initiative., 2022.
Tidal marsh distribution	Worthington, T. A., Spalding, M., Landis, E., Maxwell, T. L., Navarro, A., Smart, L. S., and Murray, N. J.: The distribution of global tidal marshes from earth observation data, <i>bioRxiv</i> , 2023.05.26.542433, https://doi.org/10.1101/2023.05.26.542433 , 2023.

Table S6. Prior gridded global soil organic carbon products for comparison

Global map comparison	
Identifier	Source
WISE30sec - 1 km resolution	Batjes, N. H.: Harmonized soil property values for broad-scale modelling (WISE30sec) with estimates of global soil carbon stocks, <i>Geoderma</i> , 269, 61–68, https://doi.org/10.1016/j.geoderma.2016.01.034 , 2016.
GSOCmap v1.5 – 1 km resolution – 30cm depth	Food and Agriculture Organization of the United Nations (FAO) and Intergovernmental Technical Panel on Soils (ITPS): Global Soil Organic Carbon Map. Technical Report, FAO, Rome, Italy, 162, 2018.
HSWD v1.21 - 1 km resolution	Food and Agriculture Organization of the United Nations (FAO), International Institute for Applied Systems Analysis (IIASA), International Soil Reference and Information Center (ISRIC), Institute of Soil Science, Chinese Academy of Sciences (ISSCAS) and Joint Research Center (JRC). 2012. Harmonized World Soil Database (version 1.2). FAO and IIASA [dataset].
SoilGrids250m v.1	Hengl, T., Mendes de Jesus, J., Heuvelink, G. B. M., Ruiperez Gonzalez, M., Kilibarda, M., Blagotić, A., Shangguan, W., Wright, M. N., Geng, X., Bauer-Marschallinger, B., Guevara, M. A., Vargas, R., MacMillan, R. A., Batjes, N. H., Leenaars, J. G. B., Ribeiro, E., Wheeler, I., Mantel, S., and Kempen, B.: SoilGrids250m: Global gridded soil information based on machine learning, <i>PLOS ONE</i> , 12, 1–40, https://doi.org/10.1371/journal.pone.0169748 , 2017.
SoilGrids250m v.2.0 at 30 cm (2020 update) – 250 m resolution – mapped unit: t/ha	Poggio, L., de Sousa, L. M., Batjes, N. H., Heuvelink, G. B. M., Kempen, B., Ribeiro, E., and Rossiter, D.: SoilGrids 2.0: producing soil information for the globe with quantified spatial uncertainty, <i>SOIL</i> , 7, 217–240, https://doi.org/10.5194/soil-7-217-2021 , 2021.
Soil carbon debt maps - 10 km resolution	Sanderman, J., Hengl, T., and Fiske, G. J.: Soil carbon debt of 12,000 years of human land use, <i>Proceedings of the National Academy of Sciences</i> , 114, 9575–9580, https://doi.org/10.1073/pnas.1706103114 , 2017.
GSDE - 1 km resolution	Shangguan, W., Dai, Y., Duan, Q., Liu, B., and Yuan, H.: A global soil data set for earth system modeling, <i>Journal of Advances in Modeling Earth Systems</i> , 6, 249–263, https://doi.org/10.1002/2013MS000293 , 2014.

Table S7. Additional land cover and ecosystem extent datasets used for zonal statistics

Datasets used for zonal statistics	
Identifier	Source
FAO GBSmap v1.0 Distribution map	Food and Agriculture Organization of the United Nations (FAO). <i>Global Map of Black Soils</i> . Rome: FAO, 2022.
SoilGrids250m 2.0 Bulk density	Hengl, T., Mendes de Jesus, J., Heuvelink, G. B. M., Ruiperez Gonzalez, M., Kilibarda, M., Blagotić, A., Shangguan, W., Wright, M. N., Geng, X., Bauer-Marschallinger, B., Guevara, M. A., Vargas, R., MacMillan, R. A., Batjes, N. H., Leenaars, J. G. B., Ribeiro, E., Wheeler, I., Mantel, S., and Kempen, B.: SoilGrids250m: Global gridded soil information based on machine learning, PLOS ONE, 12, 1–40, https://doi.org/10.1371/journal.pone.0169748 , 2017.
WWF biomes	Olson, D. M., Dinerstein, E., Wikramanayake, E. D., Burgess, N. D., Powell, G. V. N., Underwood, E. C., D'amico, J. A., Itoua, I., Strand, H. E., Morrison, J. C., Loucks, C. J., Allnutt, T. F., Ricketts, T. H., Kura, Y., Lamoreux, J. F., Wettengel, W. W., Hedao, P., and Kassem, K. R.: Terrestrial Ecoregions of the World: A New Map of Life on Earth: A new global map of terrestrial ecoregions provides an innovative tool for conserving biodiversity, BioScience, 51, 933–938, https://doi.org/10.1641/0006-3568(2001)051[0933:TEOTWA]2.0.CO;2 , 2001.
Amazon Basin	Paredes-Trejo, F., Barbosa, H., Giovannettone, J., Lakshmi Kumar, T., Kumar Thakur, M., and de Oliveira Buriti, C. Maps of the Sustainable Development Goal (SDG) indicator 15.3.1 with its sub-indicators for the entire Amazon River Basin (Version 1), https://doi.org/10.5281/zenodo.6499616 , 2022.
Cerrado biome	Schüler, J. and Bustamante, M. M. C.: Spatial planning for restoration in Cerrado: Balancing the trade-offs between conservation and agriculture, Journal of Applied Ecology, 59, 2616–2626, https://doi.org/10.1111/1365-2664.14262 , 2022.
Agricultural land - LGRIP v001 – Landsat-Derived Global Rainfed and Irrigated-Cropland Product - bands ‘irrigated’ and ‘rainfed’ agriculture were combined - 30 m resolution	Teluguntla, P., Thenkabail, P., Oliphant, A., Gumma, M., Aneece, I., Foley, D., and McCormick, R.: Landsat-Derived Global Rainfed and Irrigated-Cropland Product 30 m V001, NASA EOSDIS Land Processes Distributed Active Archive Center, https://doi.org/10.5067/Community/LGRIP/LGRIP30.001 , 2023.

Table S8. Soil organic carbon densities (t C/ha) in mangrove forests, defined by bbox in degrees

mangrove forests	soc30 (t C/ha)	soc100 (t C/ha)	bbox (min_lon, min_lat, max_lon, max_lat)
Everglades, Florida, USA	311	893	(-82.139282, 24.996016, -80.656128, 26.254010)
Futian mangroves, China	76	281	(113.612366, 22.192491, 114.428101, 22.697654)
Sundarbans mangroves, Bangladesh	58	208	(88.027954, 21.458181, 90.093384, 22.608940)
Mahd mangroves, Mumbai, India	69	216	(72.692413, 19.012138, 72.979431, 19.396011)
Edumanom mangroves, Nigeria	72	226	(4.658203, 3.962901, 8.272705, 6.424484)
Pará mangroves, Brazil	53	204	(-48.180542, -2.026555, -44.329834, -0.192260)
Mahakam mangroves, Borneo	95	329	(116.968689, -0.983228, 117.822876, -0.238952)

Table S9. Soil organic carbon densities (t C/ha) in peatlands, defined by bbox in degrees

peatlands	soc30 (t C/ha)	soc100 (t C/ha)	bbox (min_lon, min_lat, max_lon, max_lat)
Northern peatlands	121	275	(-170.156250, 34.885931, 194.765625, 79.237185)
South Hudson Bay peatlands, Canada	191	340	(-100.195313, 47.754098, -75.761719, 59.534318)
North Alaskan coast peatlands, USA	246	606	(-170.156250, 67.542167, -139.218750, 72.554498)
North peatlands, Scotlands	176	557	(-8.327637, 56.041363, -1.219482, 58.836490)
Gulf of Ob peatlands, Russia	216	516	(48.603516, 65.512963, 90.175781, 75.118222)
Tropical peatlands	57	198	(-161.015625, -23.563987, 181.757813, 23.563987)
Congo Basin, Congo	144	520	(15.183105, -6.249776, 28.300781, 5.003394)
Marajó peatlands, Brazil	76	301	(-51.866455, -2.224173, -48.240967, 0.241699)
Amazonian peatlands, Peru	102	390	(-78.596191, -7.449624, -69.499512, 0.000000)
Amazonian peatlands, Brazil	61	276	(-70.136719, -9.188870, -53.920898, 4.477856)
Borneo peatlands, Indonesia	123	422	(107.709961, -4.477856, 119.663086, 7.449624)

Figure S1. Location of ground data at 30 cm depth used in (a) the global model, (b) the peatland model, and (c) the mangrove model.

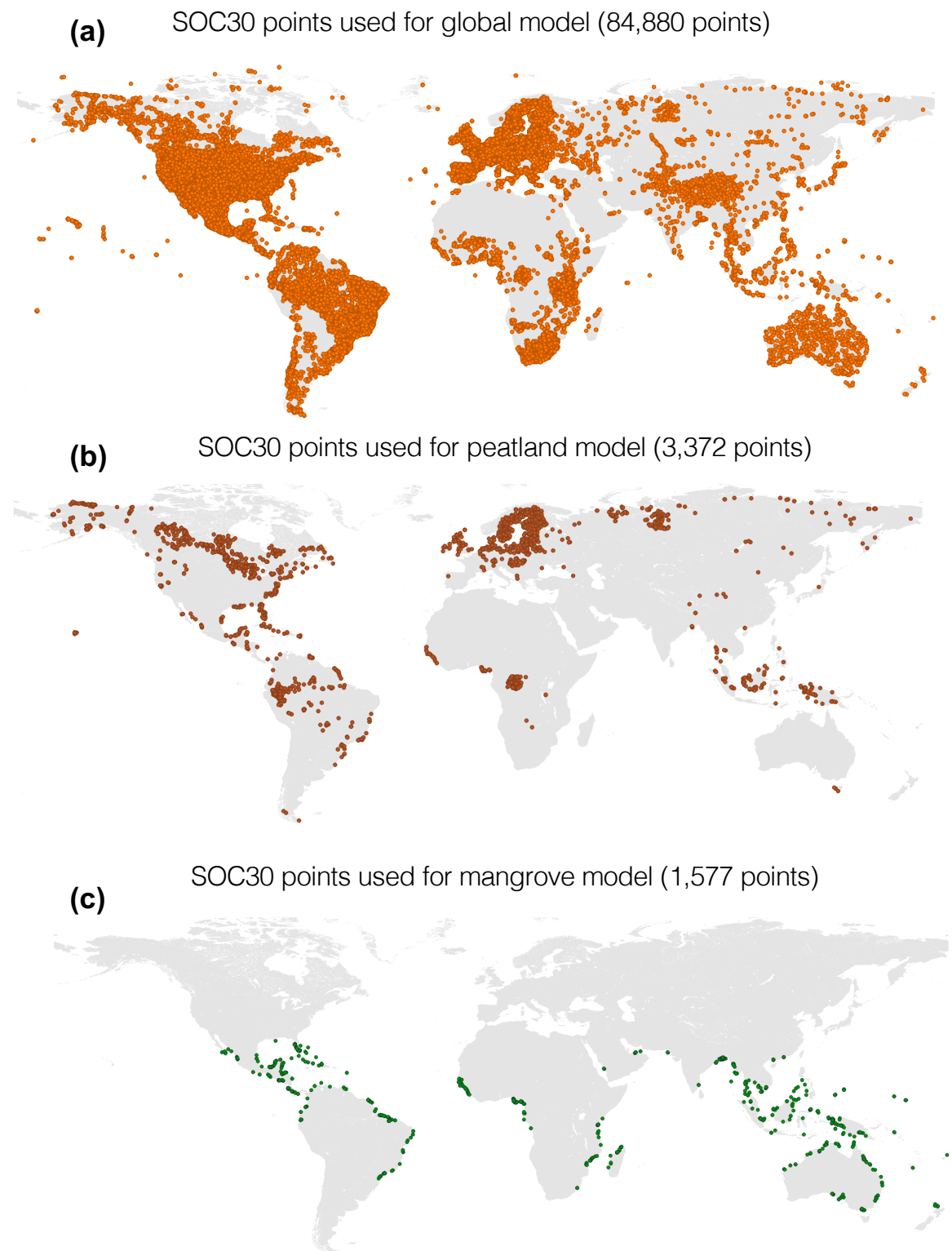


Figure S2. Location of ground data at 100 cm depth used in (a) the global model, (b) the peatland model, and (c) the mangrove model.

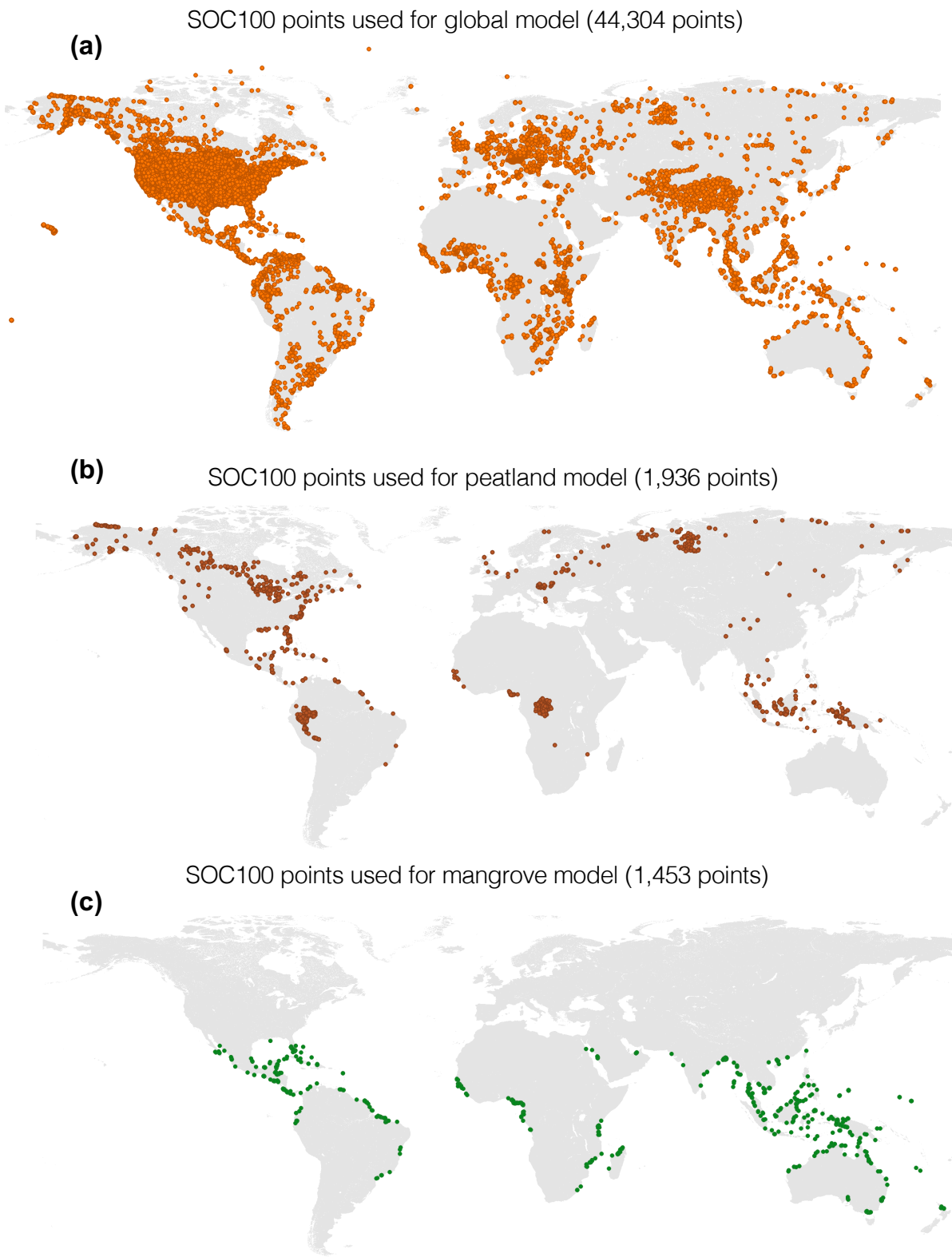


Figure S3. Predicted vs. actual SOC (t C/ha) from training data using random forest models. Panels show model performance for: (a) 30 cm global, (b) 30 cm mangrove, (c) 30 cm peatland, (d) 100 cm global, (e) 100 cm mangrove, and (f) 100 cm peatland. Performance metrics are included for each model.

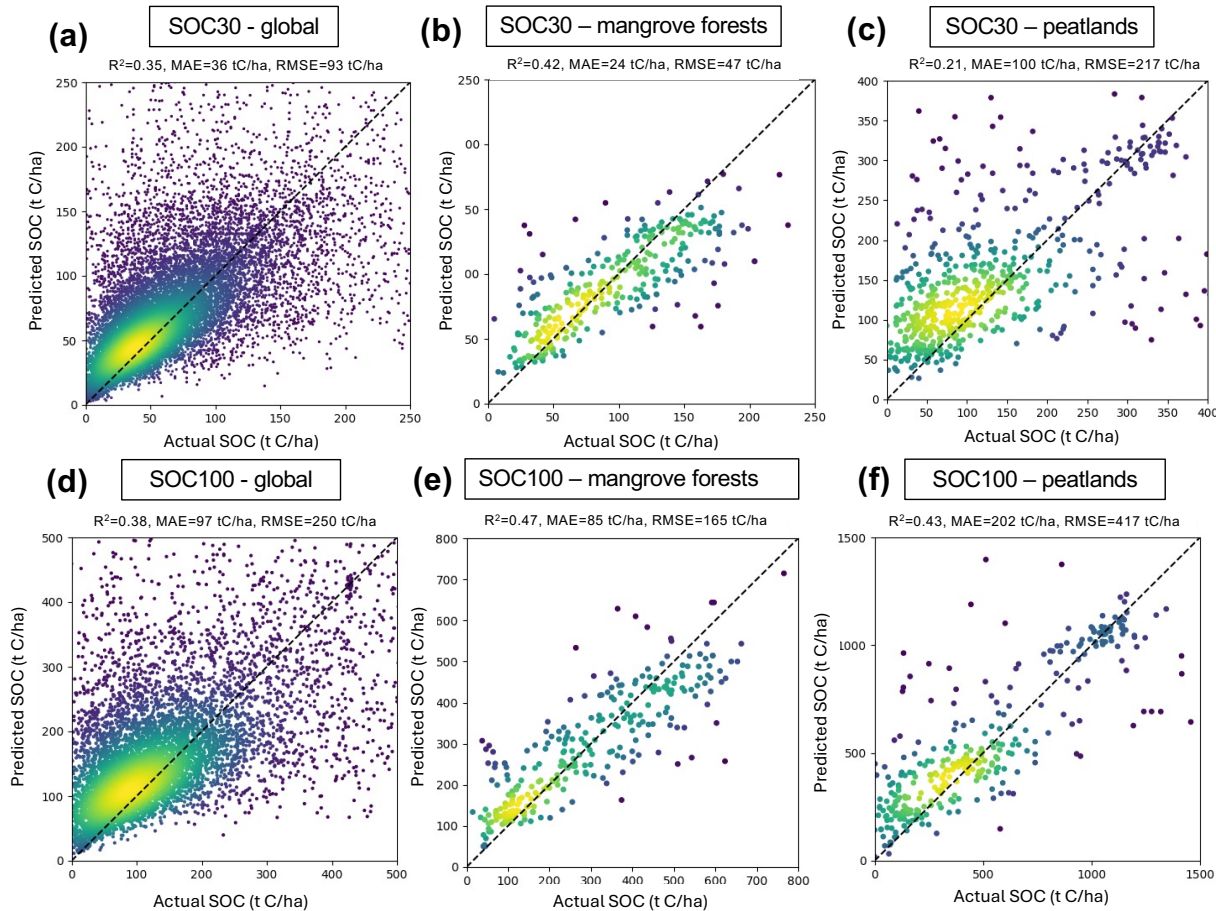


Figure S4. Binned predicted vs. actual SOC (t C/ha) for 30 cm and 100 cm depths, before and after bias correction. Panels show: (a) 30 cm pre-correction, (b) 30 cm post-correction, (c) 100 cm pre-correction, and (d) 100 cm post-correction.

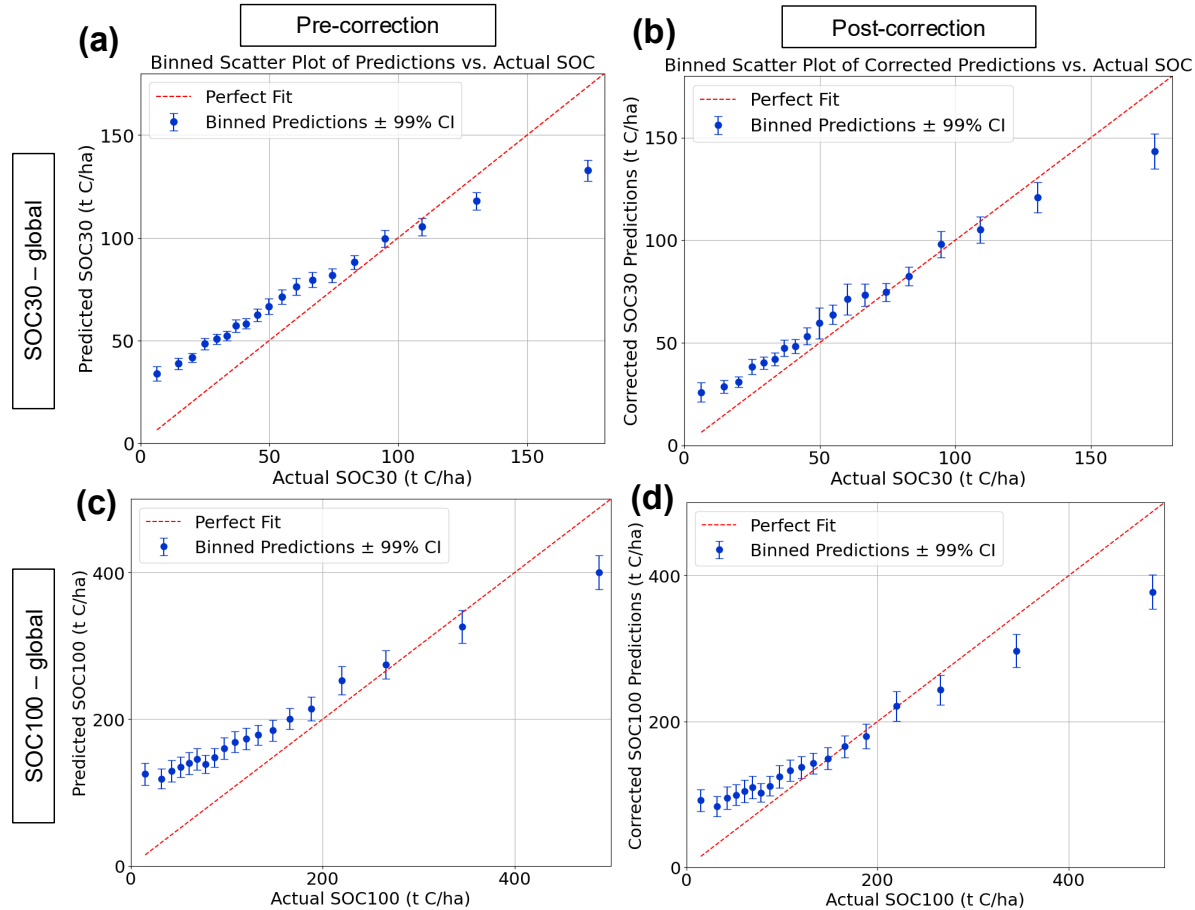


Figure S5. Residuals by actual SOC bins (t C/ha) for SOC30 and SOC100 before and after bias correction. Panels show: (a) 30 cm pre-correction, (b) 30 cm post-correction, (c) 100 cm pre-correction, and (d) 100 cm post-correction.

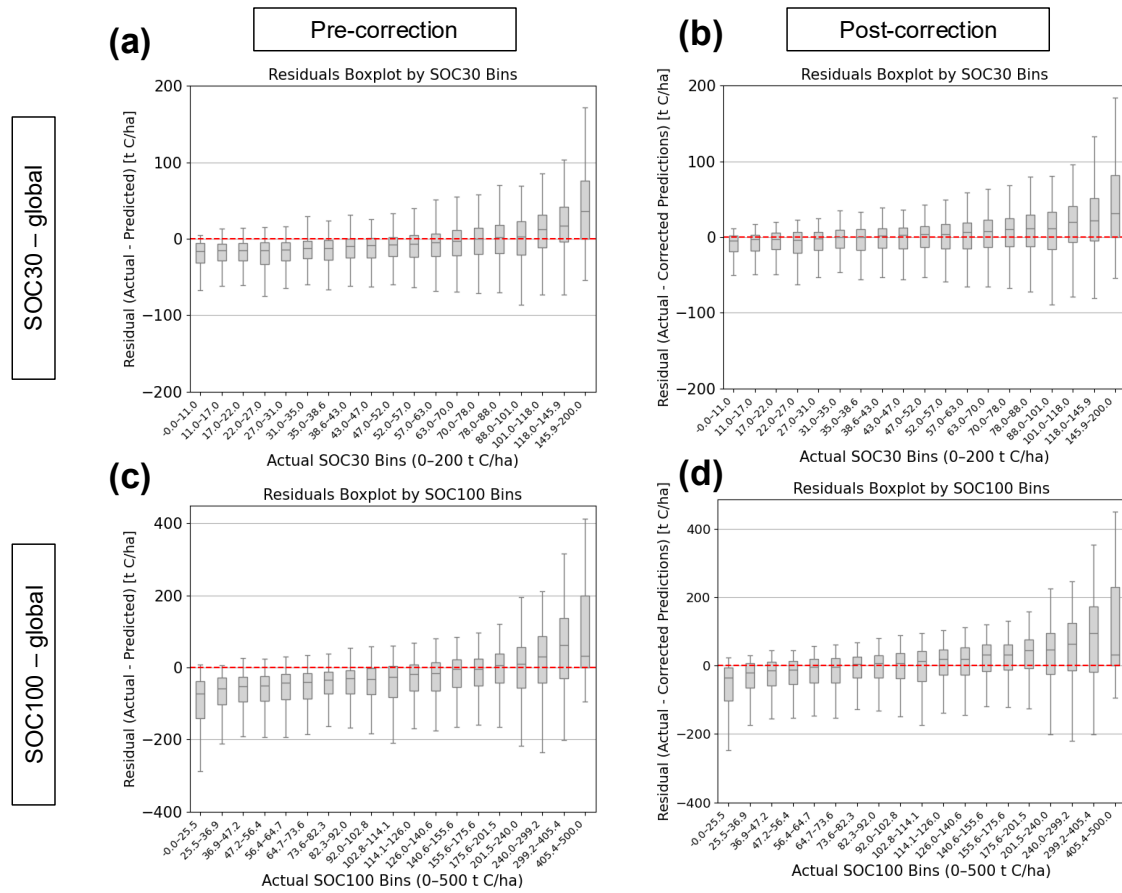


Figure S6. Pixel-based standard deviation at (a) 30 cm depth and (b) 100 cm depth

